deposits are associated with craters Greenaway and Stanton and cover about 100 times the area of each crater, 2.6 and 3.4 million km^2, or 0.6% and 0.8% of the total surface area of Venus respectively. Assuming that extended ejecta is contemporaneous with the parent crater as a given, it follows logically that extended ejecta deposits are local time-stratigraphic markers. Such extended units will not improve temporal resolution (i.e., they will not give a better constraint on absolute time, since they are present around a subset of the already small, spread-out crater population). However, the extended deposits will improve the spatial domain significantly, as the deposits cover up to millions of square kilometers in a single geologic instant, allowing for determination of relative time progressions in many localities.

A reconnaissance survey of 336 craters (about 40% of the total population) was conducted. About half the craters examined were located in and around the Beta-Atla-Themis region, and half were spread over the western hemisphere of the planet. The survey was conducted using primarily C1-MIDR images. The preliminary survey shows (1) Of the 336 craters, 223 were found to have extended ejecta deposits. This proportion is higher than that found in other Venus crater databases by up to a factor of 2 [12]. (2) 53% of all extended ejecta craters were unambiguously superimposed on all volcanic and tectonic units. Figure 1 shows a representative example of this group. Crater Annia Faustina's associated parabolic ejecta deposit is clearly superimposed on volcanic flows coming from Gula Mons to the west (Gula is not shown). Parabola material from Faustina has covered the lava flows, smoothing the surface and reducing its specific backscatter cross section. The stratigraphy implies that the parabola material is the youngest observable unit in the region. (3) 12% of extended ejecta deposits are superimposed by volcanic materials. Figure 2 shows a typical example. Crater Hwangcini has extended ejecta that has been covered by volcanic flows from a dome field to the northwest, implying that the volcanic
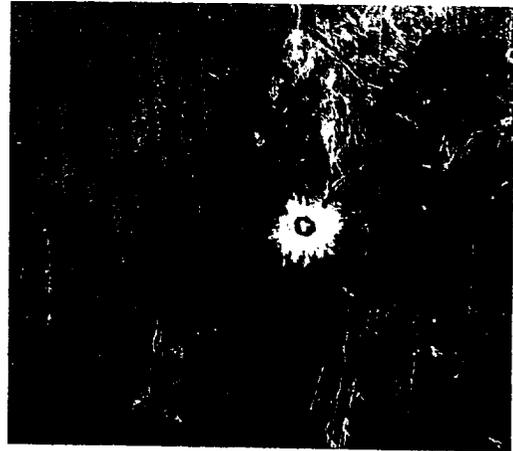
Fig. 2. Crater Hwangcini, 31 km in diameter with a low cross-section halo of about 230 km diameter that has been embayed to the west by flows associated with the dome field there. The crater is located northwest of Thetis Regio.

units were emplaced subsequent to the ejecta deposit and are the youngest units in the locality. (4) It is difficult to determine the stratigraphic relationships of the remaining extended ejecta deposits in SAR at C1-MIDR resolution. Examination of higher resolution images and application of the other Magellan datasets in a systematic manner should resolve most of the ambiguous cases.

Results from the preliminary survey indicate that extended ejecta deposits are effective time-stratigraphic markers for their localities. If stratigraphic relationships between the deposits and surrounding units are studied on a case-by-case basis over the whole planet, they should provide useful constraints on Venus history and development of the surface through time. The continuation of this research will expand the study to include the entire crater population and the Magellan emissivity, altimetry, reflectivity, and rms slope datasets.

References: [1] Phillips R. J. et al. (1992) JGR, submitted. [2] Schaber G. G. et al. (1992) JGR, submitted. [3] Izenberg N. R. et al. (1992) LPSC XXIII, 591–592. [4] Arvidson R. E. et al. (1992) Eos, 73, 161–169. (5) Head J. W. et al. (1992) JGR, submitted. [6] Shoemaker E. M. (1962) Physics and Astronomy of the Moon (Z. Kopal, ed.), 283–359, Academic, New York. [7] Wilhelms D. E. (1987) U.S. Geol. Surv. Prof. Pap. 1348. [8] Arvidson R. E. et al. (1991) Science, 252, 270–275. [9] Vervack R. J. and Melosh H. J. (1991) Eos, 72, 289. [10] Campbell D. B. et al. (1992) JGR, submitted. [11] Phillips R. J. et al. (1991) Science, 252, 249–252. [12] Herrick R. R. (1992) personal communication.

N93-14328

LONG-TERM VARIATIONS IN ABUNDANCE AND DISTRIBUTION OF SULFURIC ACID VAPOR IN THE VENUS ATMOSPHERE INFERRED FROM PIONEER VENUS AND MAGELLAN RADIO OCCULTATION STUDIES.

J. M. Jenkins[1] and P. G. Steffes[2], [1]SETI Institute, NASA Ames Research Center, Moffett Field CA 94035, USA, [2]Georgia Institute of Technology, Atlanta GA 30332, USA.

Radio occultation experiments have been used to study various properties of planetary atmospheres, including pressure and temperature profiles, and the abundance profiles of absorbing constitu-

Fig. 1. Crater Annia Faustina, located east of Gula Mons. The crater is 22 km across, and the parabola is 6630 km long and and 720 km across. Parabola material from Faustina clearly darkens lava flows from Gula Mons where it appears that centimeters to decimeters of covering ejecta material reduces the radar wavelength scale roughness of the surface.
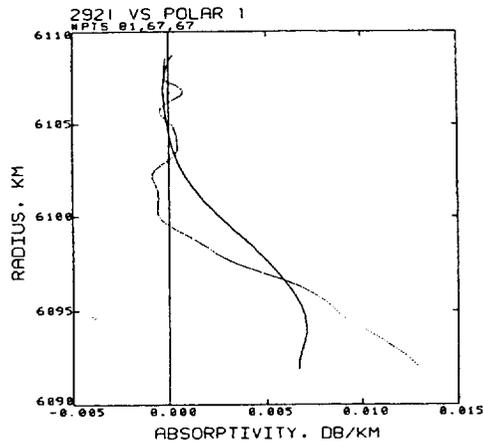
Fig. 1. Absorptivity profiles for near-polar PVORO experiments from 1979 (dotted line) and 1986 (solid line). Since $H_2SO_4(g)$ is the dominant 13-cm absorber in the Venus atmosphere, this plot suggests that the abundance of $H_2SO_4(g)$ decreased form 1979 to 1986 in the high northern latitudes.

ents in those planetary atmospheres. However, the reduction of amplitude data from such experiments to determine abundance profiles requires the application of the inverse Abel transform (IAT) and numerical differentiation of experimental data. These two operations preferentially amplify measurement errors above the true signal underlying the data. A new technique for processing radio occultation data has been developed that greatly reduces the errors in the derived absorptivity and abundance profiles. This technique has been applied to datasets aquired from Pioneer Venus Orbiter radio occultation studies and more recently to experiments conducted with the Magellan spacecraft.

While primarily designed for radar studies of the Venus surface, the high radiated power (EIRP) from the Magellan spacecraft makes it an ideal transmitter for measuring the refractivity and absorptivity of the Venus atmosphere by such experiments. Two transmitter frequencies were used: 2.3 GHz and 8.4 GHz (13 cm and 3.6 cm, respectively), and the measurements were made during spacecraft ingress on three consecutive orbits on October 5, 1991. Since the stability of the spacecraft transmitted frequencies is critical for accurate retrieval of atmospheric properties from the signals recorded on Earth, the spacecraft transmitter was locked to a 2.1-GHz uplink from DSS-43 (Tidbinbilla, Australia), which also received the signals. Because of the high gain of the spacecraft antenna, and the large ray bending in the deep Venus atmosphere, a spacecraft tracking maneuver was designed to keep the spacecraft antenna pointed in the direction of the refracted ray path back to Earth. This tracking maneuver, plus the high EIRP of the Magellan transmitter, yielded 3.6-cm refractivity and absorptivity profiles down to altitudes below 36 km, and 13-cm profiles to altitudes below 34 km (above a radius of 6052 km). These experiments probed much deeper in the atmosphere than previous radio occultation experiments conducted with the Pioneer Venus Orbiter, which reached altitudes of 54 km at 3.6 cm, and 40 km at 13 cm.

The longevity of the Pioneer Venus Orbiter has made it possible to study long-term changes in the abundance and distribution of sulfuric acid vapor, $H_2SO_4(g)$, in the Venus atmosphere between 1979 and 1992. The abundance of $H_2SO_4(g)$ can be inferred from vertical profiles of 13-cm absorptivity profiles retrieved from radio occultation experiments [1]. Data from 1979 and 1986–87 suggest

that the abundance of $H_2SO_4(g)$ at latitudes northward of 70° decreased over this time period (see Fig. 1). This change may be due to a period of active volcanism in the late 1970s followed by a relatively quiescent period, or some other dynamic process in the Venus atmosphere. While the cause is not certain, such changes must be incorporated into dynamic models of the Venus atmosphere.

Potentially, the Magellan spacecraft will extend the results of Pioneer Venus Orbiter and allow the continued monitoring of the abundance and distribution of $H_2SO_4(g)$ in the Venus atmosphere, as well as other interesting atmospheric properties. Without such measurements it will be difficult to address other issues such as the short-term spatial variability of the abundance of $H_2SO_4(g)$ at similar latitudes in Venus atmosphere, and the identities of particles responsible for large-scale variations observed in NIR images [2].

References: [1] Jenkins J. M. and Steffes P. G. (1991) *Icarus*, 90, 129–138. [2] Ragent B. et al. (1991) *Bull. A.A.S.*, 23, 1192.

N93-14329

VARIATIONS IN LITHOSPHERIC THICKNESS ON VENUS.
C. L. Johnson and D. T. Sandwell, Scripps Institution of Oceanography, La Jolla CA 92093-0208, USA.

Recent analyses of Magellan data have indicated many regions exhibiting topographic flexure [1,2,3]. On Earth, flexure occurs at oceanic trenches and around seamounts. On Venus, flexure is associated predominantly with coronae [1,3] and the chasmata within Aphrodite Terra [2,3]. Modeling of these flexural signatures allows the elastic and mechanical thickness of the lithosphere to be estimated. In areas where the lithosphere is flexed beyond its elastic limit the saturation moment provides information on the strength of the lithosphere. Modeling of 12 flexural features on Venus has indicated lithospheric thicknesses comparable with terrestrial values. This has important implications for the venusian heat budget.

Model: Flexure of a thin elastic plate due simultaneously to a line load on a continuous plate and a bending moment applied to the end of a broken plate is considered. The mean radius and regional topographic gradient are also included in the model. Features with a large radius of curvature were selected so that a two-dimensional approximation could be used. Comparisons with an axisymmetric model were made for some features to check the validity of the two-dimensional assumption. The best-fit elastic thickness was found for each profile crossing a given flexural feature. In addition, the surface stress and bending moment at the first zero crossing of each profile were also calculated.

Results: Flexural amplitudes and elastic thicknesses obtained for 12 features vary significantly. Three examples of the model fitting procedure are shown in Fig. 1, where the solid line is the data and the dashed line the best-fit model. The lowest elastic thickness was obtained at Nishtigri Corona (8–12 km) where the flexural amplitude is low (0.4 km). Nightingale Corona was typical of several other areas with elastic thicknesses in the range 18–25 km and a flexural amplitude of about 0.8 km. At W. Dali Chasma the lithosphere appears very thick (25–40 km) and the flexural amplitude is large (3 km); a similar result was obtained for other areas in Aphrodite Terra. However, the amplitude of the flexure at Artemis and Latona Coronae and at the chasmata of Aphrodite Terra is extremely large and it is likely that in these areas the lithosphere is flexed beyond its elastic limit. In some regions of extreme curvature it was not possible to model the topography to the base of the flexural moat (e.g., W. Dali Chasma, Fig. 1); this is probably due to extensive faulting. SAR images of several areas exhibiting flexure